Landsat TM data processing system at EOC/NASDA

S.Yamamoto,
C.Ishida
and
K.Tachi

National Space Development Agency of Japan
Earth Observation Center(EOC)
Japan

II/4

Abstract

Japanese TM data processing system,which is based upon V 90/50 host computer(32 bits,4 MBytes main memory) and array processor(AP 120 B), was installed at Earth Observation Center/National Space Development Agency of Japan (EOC/NASDA) in Sep. 1983.

We don't have TM descending data over Japan . However, prelimimary TM data evaluation experiments were made using TM HDT's which were provided by NASA and NOAA.

I. Introduction

The development of TM data processing system started in 1981 and the hardware construction finished in Aug.1983. The installation and adjustments of the system took place from Aug. to Sep. and acceptance tests were conducted by the end of Sep. 1983.

The total system became functional then,but verification of radiometric and geometric correction accuracies has been suspended until Landsat5 TM data over Japan become available.

Fortunatlly some TM HDT's were provided by NASA and NOAA, so we have continued prelimimary evaluation experiments on TM data characteristics.

This paper describes our TM data processing hardware and software system and also summarizes the result of the TM data evaluation experiments in our center.

II. Hardware construction for TM processing system

As is shown in Fig.1, TM data processing system consists of two independant subsystems, i.e. TM IDPS(TM Image Data Processing Subsystem) and TM PGS (TM Products Generation Subsystem).

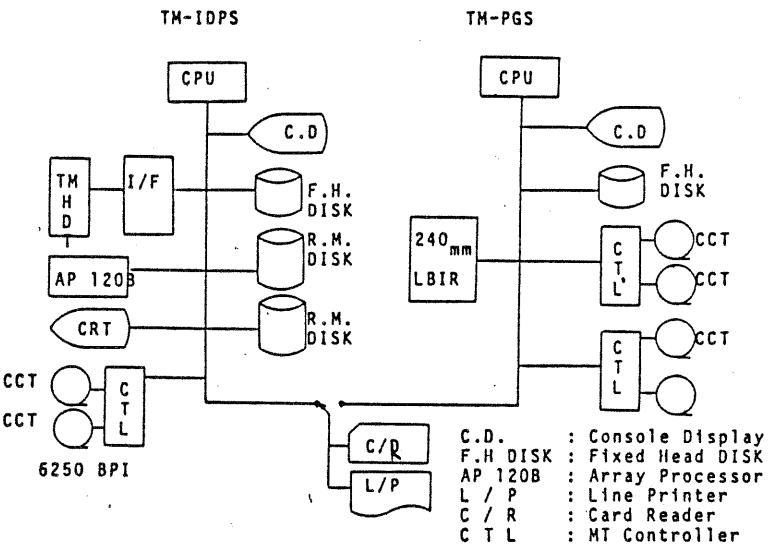

Fig. 1 TM IDPS & TM PGS Hardware structure

TM IDPS(left in fig.1) reproduces TM data from HDT and performs radiometric and geometric corrections and out put the data into CCTs. TM IDPS has two removable disks(300 MBytes for each disk) to store forward and reverse scan data,respectively. TM frame synchronizer(TMFS) and TM control equipment (TMCE) were developed for feeding and decommutating TM data.

TM PGS is for feeding the TM data from CCTs and expose the TM image onto 240 mm film.In order to produce original latent film , 240 mm Laser Beam Image Recoder(LBIR) was developed.

Both subsystems are based upon 32 bits host computer. System performances of TM IDPS and TM PGS are summarized in table 1 .

Table 1 System performance of TM IDPS and TM PGS

TM IDPS		TM PGS	
Processing mode	Uncorrected Bukl Precision Precision registration	Film Pixel/scan	240 mm roll film 8 K(8192pixels/line
Processing accuracy	Bulk : 1000 m Precision : 1 pixel	Pixel interval Resolution	28.5 micro meter 8 bit (256 levels)
Processing time	Bulk : 90 min Precision : 120min	Light source (Laser)	Blue : He Cd Green : Ar Ion Red : He Ne
Map projection CCT format	UTM / SOM BSQ / BIL		
CCT recording density	6250 BPI		
Output mode	Full scene/ subscene		

III. TM data processing software

TM data processing software consists of four stages, which are designated as pass 0, pass 1 pass 2 and pass 3 respectively(See Fig.2). General descriptions of each processing stage are presented in the following.

(1) pass 0

Pass 0 is for reproducing HDT recorded with satellite image data and feeding the image data, calibration data, DC restore data and PCD(payload correction data) into disk memories.

Using ephemeris data which are telexed from NASA , compute satellite orbit information and determine HDT reading start time. Next,feed PCD into a disk memory as they are reproduced with real time speed, and then feed image data, calibration data as they reproduced with 1/16 speed.

Histogram data which are generated by TMCE (TM control equipment) are also stored at the same time in two RM disks.

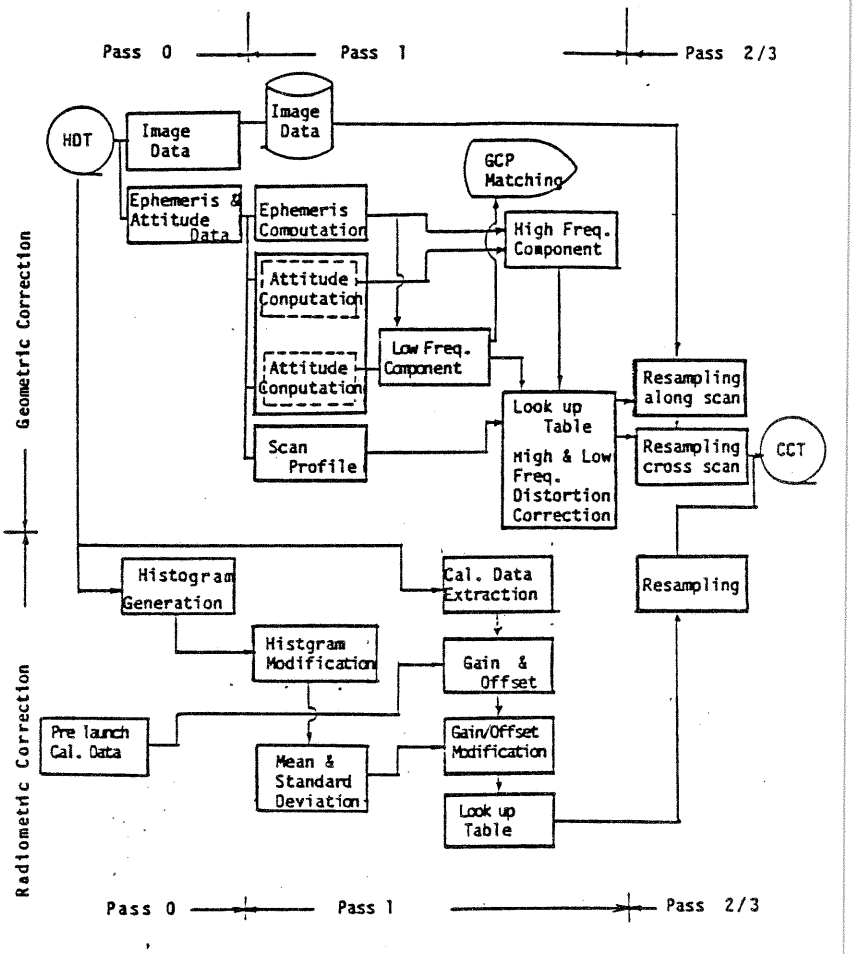

Fig. 2 Flow chart of geometric & radiometric correction

(2) pass 1

Pass 1 computes radiometric and geometric correction coefficients for removing distortions due to sensor responsivity characteristics and satellite attitude changes and outputting the image data by designated mapping projection method. Satellite position, velocity and attitude are computed from the edited PCD data. In case of missing ephemeris data points, the missing data are interpolated with adjacent data points by the VINTI's ephemeris generation method.

Radiometric correction coefficients are computed from histgram data, calibration data and DC restore data,and then radiometric correction table is generated in Pass 1. On the other hand gemetric correction coefficients are computed considering high and low frequency component of S/C attitude deviation.

(3) pass 2

Applying radiometric and geometric correction coefficients, which are generated in Pass 1, to the uncorrected imge data, execute radiometric and geometric corrections then output the corrected image data into CCT's.
Pass 2 also output the uncorrected imge data into CCT s together with supplementary data.

(4) Pass 3

Pass 3 is for generating BIL(Band Interleaved by Line) CCT's by reformatting data from BSQ (Band Sequensial) CCT'S.

IV. Preliminary TM data evaluation experiments

Preliminary evaluation experiments on TM data characteristics were made with the following items.

(1) Relative detector responsivity evaluation
(2) Calibration lamp data analysis
(3) Scan direction radiance difference and relative radiometric correction
(4) Coherent nois analysis
(5) PCD(Payloard Correction Data) analysis

General procedure and early results for each items indicates in the following sections.

(1) Relative Detector Responsivity Evaluation

Detector relative gain and offset were computed from image data histogram and compared with those computed from the pre-launch gain and offset values which were provided by NASA. Primary objectives of this analysis are to evaluate TM detector responsivity stability and to examine the applicability of the pre-launch responsivity data to the radiometric correction. Several scenes in path 20 (received on July 25, 82), path 15 (Nov 2, 82) were used for the analysis.

The following results were obtained.
(a) Stability of relative gain and offset depends upon band No. and scene. Band 1 is most variable with scene, while Bands 3 and 4 exhibit most stable responsivity characteristics. Relationship between the pre-launch relative responsivity and the image-derived post-launch relative responsivity is shown in Fig. 3. From the figure, it is seen that the responsivity change during the period is fairly small.
(b) Linearity between the pre-launch responsivity and post-launch responsivity also varies with band No. Here again Bands 3 and 4 exhibited good linearity. Correlation rate of relative gain varied around 0.90 - 0.95 for Bands 3 and 4 and 0.6 - 0.9 for other bands. Relative offset correlation rate varied 0.7 - 0.9 for Bands 3 and 4 and 0.3 - 0.8 for other bands. As shown in Fig.3, in general, good linearity holds between the pre-launch and post-launch responsivity.

GAIN
(B4/D8)

OFFSET
(B3/D5)

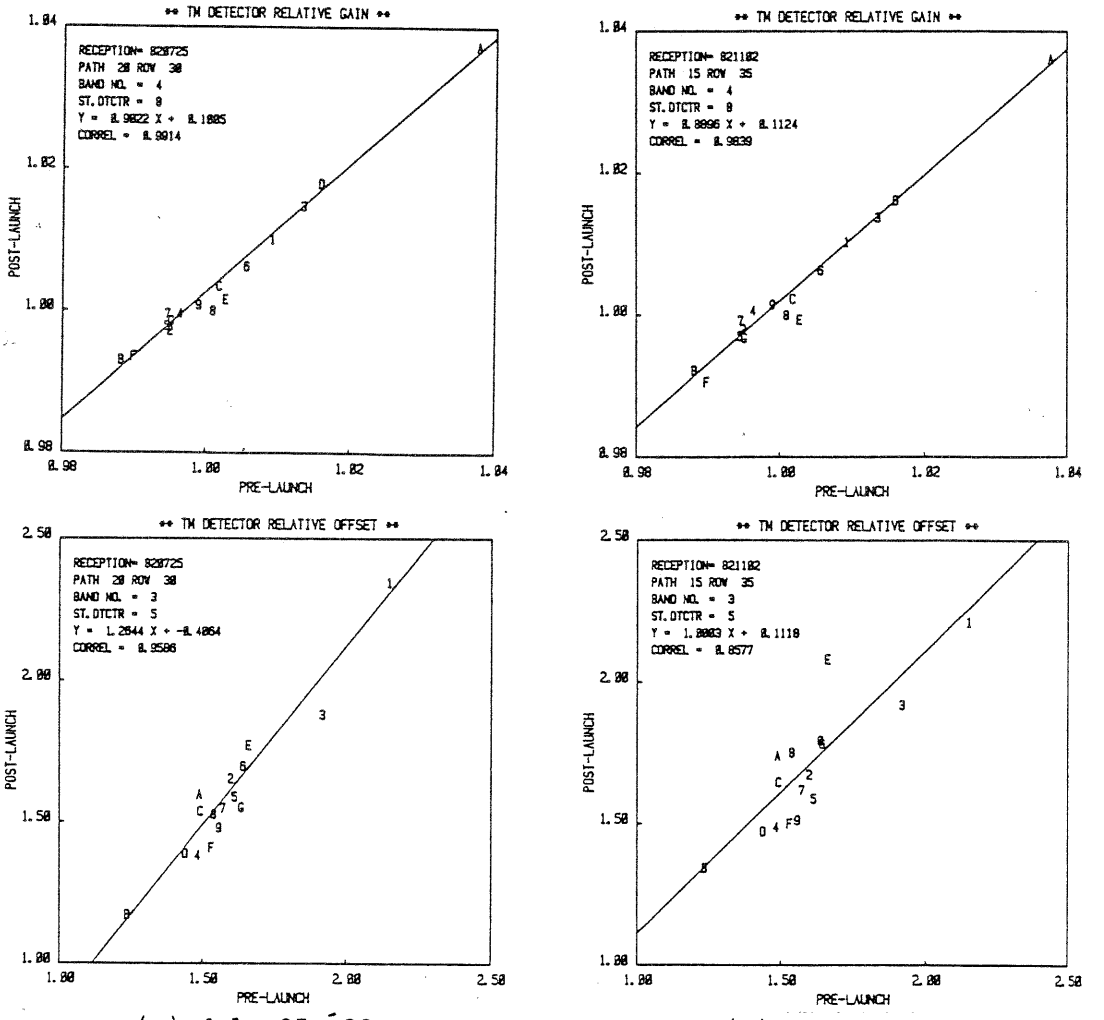

(a) July 25, 82 (b) Nov 2, 82

Fig. 3 Relationship between pre-launch detector responsivity and post-launch detector responsivity.

(2) Calibration Lamp Data Analysis

Internal calibration lamp data profile for each detector was obtained by averaging data within every scan. By monitoring the data profile change, an attemp was made to evaluate the calibration lamp data stability, linearity and other characteristics.

Monitoring was made for two scenes; (a) Detroit, July 25, 82, (b) Chicago, Oct 25, 82. An example of the calibration lamp data profile (data (b), Band 4 Detector 8) is shown in Fig. 4. Features to be noticed are overshootings which appear when the calibration lamp status transition occurs and periodic level variation within each lamp status. Large overshooting (up to 20%) of calibration lamp data was observed for Bands 1 to 4, while small overshooting (up to 5%) of calibration lamp data were seen in Bands 5 and 7. It is considered due to the different detector types; i.e. Si photodiode for Bands 1 to 4 and InSb photodiode for Bands 5 and 7. Periodic data level changes occur to all the bands with periodicity of 6 scans. The exact cause of this periodic data level change is not known.

Relationship between the averaged calibration value of each lamp status and then lamp radiance is shown in Fig. 5. As shown in the figure, a good linearity holds between the input radiance and then output calibration lamp data. In the comparison of calibration data profiles between data (a) and data (b), some decrease in gain was observed. The similar decrease in calibration lamp level was observed in all bands. Monitoring should be continued to decide whether the decrease in gain is due to the detector responsivity change or calibration lamp radiacne change.

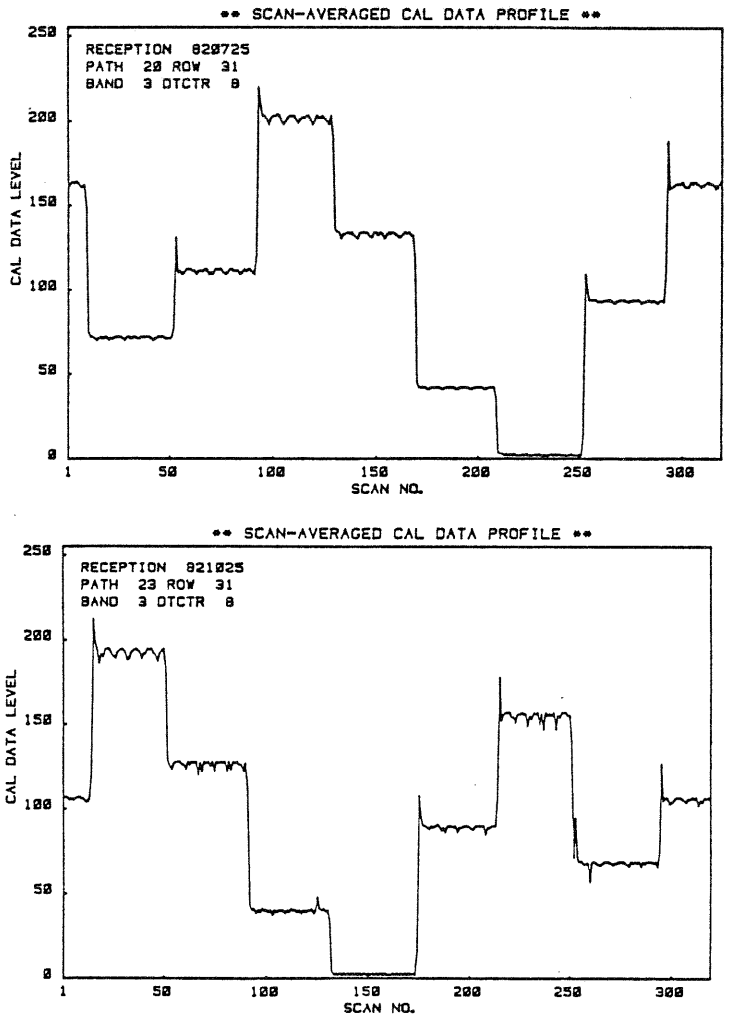

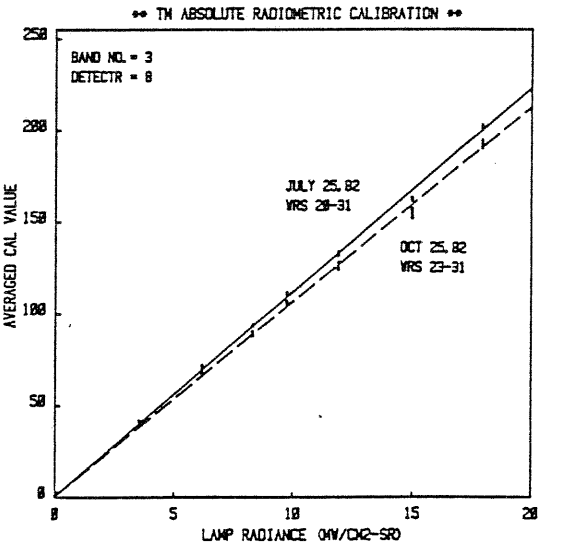

Left:Fig.4 Scan-averaged calibration data profile for a scene.
upper: Detroit, July 25, 82
lower: Chicago, Oct 25, 82

Right:Fig.5 Relationship between lamp radiance and calibration value.
(Band 3 Detector 8)

(3) Scan-direction Radiance Difference and Relative Radiometric Correction

Visual inspection of raw TM image indicates the existance of average difference between the forward and reverse scans. The cases of (a) Chicago, Oct 25, 82 and (b) Washington, Nov 2, 82 are shown in Fig. 6 for Band 4 in terms of mean and S.D. values of respective image histogram of forward and reverse scans. From the similar analysis with other scenes, it is known that the image statistics difference due to scan direction has scene dependence. The cause of the phenomenon is not known well.

Above mentioned difference in radiometric characteristics due to scan direction indicates the necessity of separate radiometric correction for forward and reverse scan data. Such an exeperiment was made using data of Chicago, Oct 25, 82. Enlarged resultant images are shown in Fig. 7
(a) is the image corrected by conventional method, in which forward and reverse scan data are handled equally for each detector, while (b) is the image which was applied with a scan-direction separate radiometric correction, i.e. applying radiometric corrections to forward and reverse scan data separately using the forward and reverse scan data statistics, respectively.
The effect of removing scan-direction average radiance by scan-direction separate radiometric correction is clearly shown. It turned out that the scan-direction separate radiometric correction is effective for all bands.

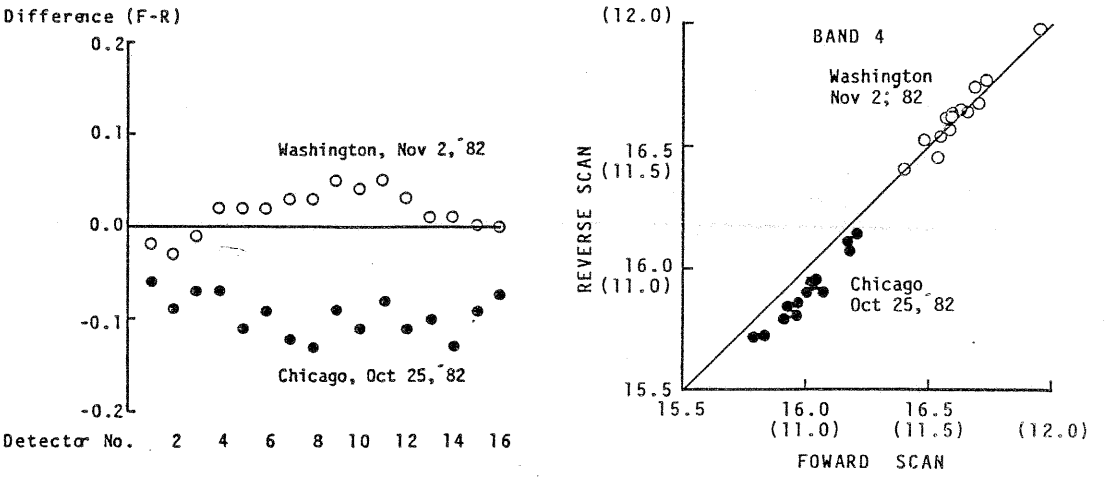

Fig.6 Scan-direction radiance difference for Band 4 detectors
Left: Mean difference, Right: Standard Deviation

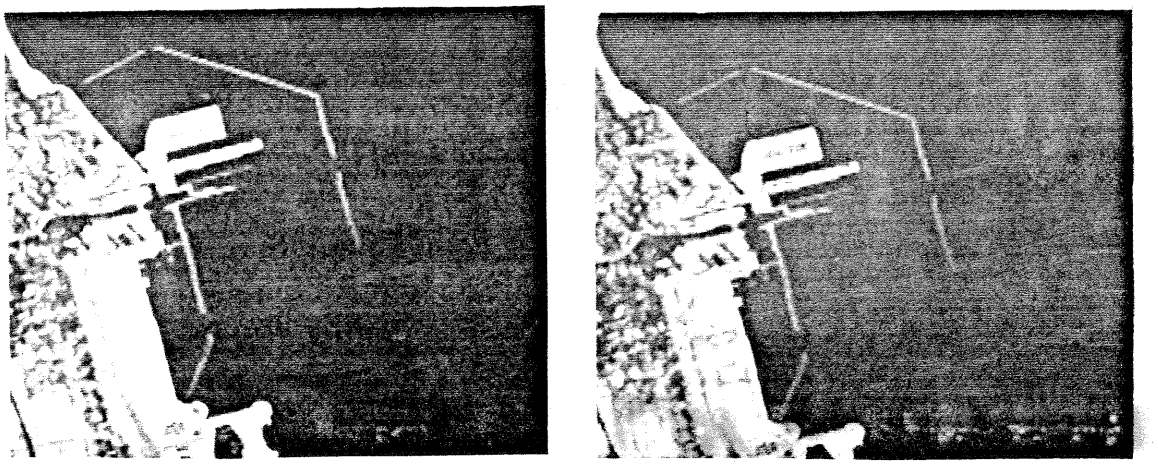

(a) Conventional correction (b) Scan-direction separate correction
Fig.7 Relative radiometric correction (Band 4, enlarged)

(4) Coherent Noise Analysis

In MSS image of Landsat 4, coherent noise exists in a low-level uniform area such as sea surface. Investigation was made to see whether the same phenomenon is found in TM image or not by Fourier analysis. Data used in the analysis were (a) Detroit, July 25, 82 and (b) Chicago, Oct 25, 82. In the analysis, ocean areas with 256 x 256 pixel size were selected as test sites and applied with Fourier transform. In Fig. 8 shown are raw image, its Fourier spectrum image, pixel direction (horizontal) Fourier spectrum and line direction (vertical) Fourier spectrum.

As shown in (a), coherent noise component with a wave number of 17.8 (wavelength 14.3 pixel) is oberved in pixel direction. While in Fig. 8.(b), another coherent noise component with a wave number of 77 (wavelength 3.3 pixel) appears. In both scenes, the same frequency components existed in all bands. The magnitudes of the first and second coherent noise components are 0.5 level (p-p) and 0.2 level (p-p), respectively. On the other hand, in the line direction (vertical) Fourier spectrum, frequency components with wave numbers of 8 and 16 (wavelength 32 and 16 pixels) exist, which are due to "striping" (intra-detector responsivity difference) and "banding" (intra-scan radiance difference) in the image.

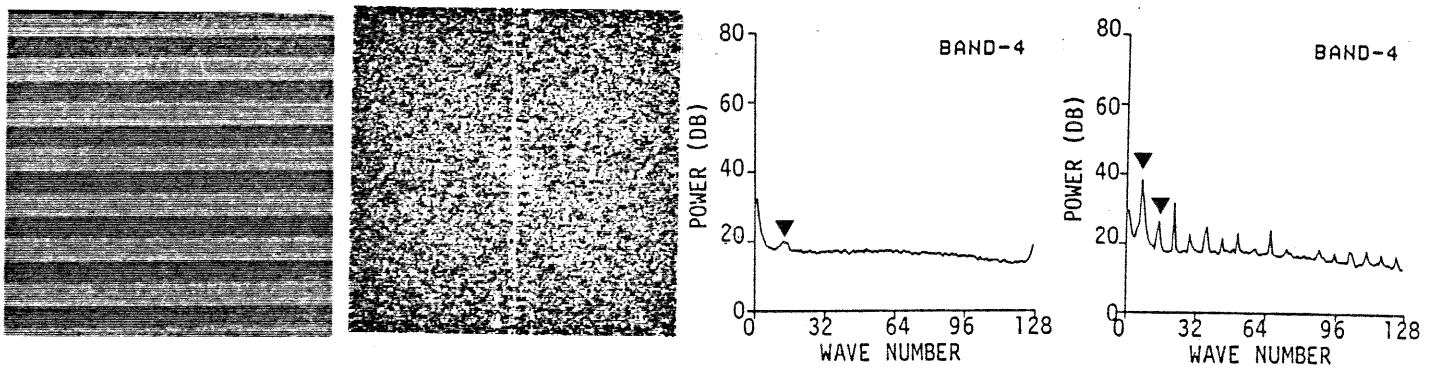

(a) Detroit, July 25, 82

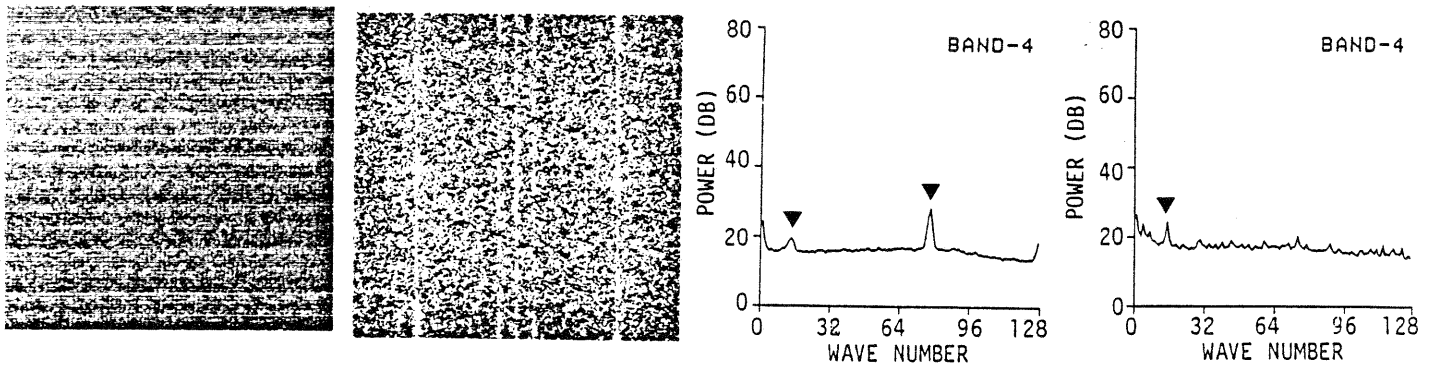

(b) Chicago, Oct 25, 82

Fig. 8 TM Fourier spectrum analysis (Band 4)
from left: raw image, two-dimensional Fourier spectrum image, pixel-direction Fourier spectrum, line-direction Fourier spectrum

(5) PCD analysis

Payload Correction Data ,giving spacecraft attitude information, contains Euler parameters,Gyro data, Gyro drift data and ADS(Angular Displacement Sensor)data.

By analyzing these data, satellite attitude characteristics will be evaluated.

At first we extracted 512 samples of Gyro data every 64 msec and 16384 samples of ADS data every 2 msec for each axis. Second, applying one dimensional Fourier transform to raw Gyro and ADS data, power spectrums are computed.

Fig.9 shows ADS data for roll,pitch and yaw axis and Fig. 10 shows power spectrums for each axis,respectively.

As shown in Fig. 10, one dimensional Fourier transforms of ADS data indicates that dominant source of high frequent attitude deviation are 7 Hz 13.6 Hz,63 Hz and 68 Hz for roll axis and 2.4 Hz ,21 Hz and 63 Hz for pitch axis. On the other hand for yaw axis 21 Hz and 68 Hz osclation are dominant.

The result of the Fourier analysis sugests that TM and MSS scanning mirrors have an important effects on high frequent attitude deviation of spacecraft.

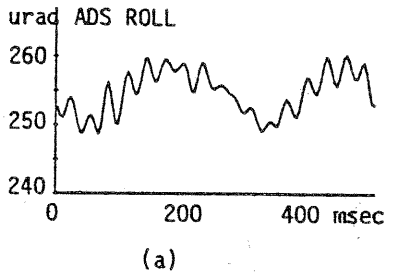

(a)

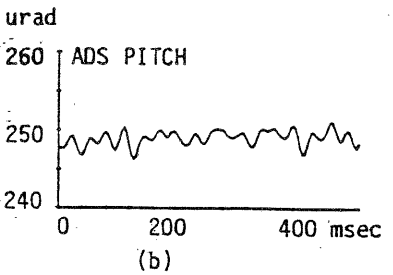

(b)

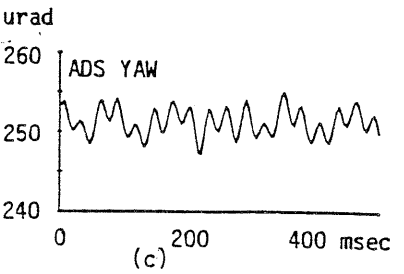

(c)

Fig. 9 ADS data
(Chicago,1982.10.25)

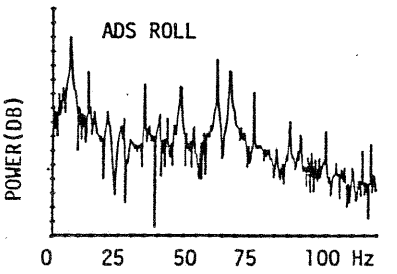

(a)

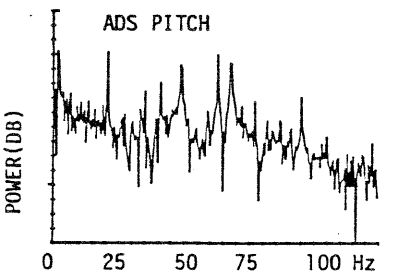

(b)

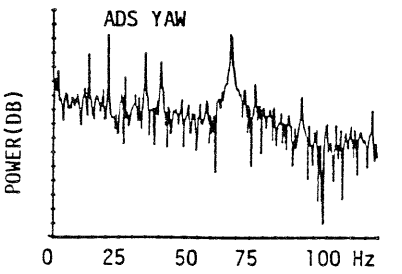

(c)

Fig. 10 power spectrum of ADS
(Chicago,1982.10.25)

V. Concluding remarks

In this paper, general discription of Japanese TM data processing system and some preliminary results of TM data evaluations are presented. The TM data processing system is undergoing final adjustments using NASA & NOAA provided TM HDTs. In parallel with the system adjustments, TM data evaluation is being promoted with a view to reflecting the results to the improvement of the system correction accuracies.

In the TM data evaluation, it was found that responsivity of detector is considerably stable and the pre launch responsibity data is applicable to correct radiometric distortion.

Calibration lamp data analysis indicated stable characteristics and the radiometric correction method based upon the internal calibration system will be developed.

Revealed average radiance difference between forward and reverse scans indicated the necessity of scan direction separate radiometric correction. The experiment of separate radiometric correction showed good results in removing the radiance difference. The separate radiometric correction will be adopted to the daily processing system.

It was seen that TM data also contain coherent noises likewise MSS data. The effect of the noise to the data utility should be evaluated.

For geometric correction, the analysis of PCD data showed a significant relationship between the high frequent spacecraft oscillations and the scanning of TM and MSS mirrors. Such analysis will help understanding the nature of geometric errors,thereby refining the geometric correction method.

We very much appreciated Mr. Iijima (Remote Sensing Technology Center of Japan) and Mr. Nakahata (Hitachi,Ltd.) for their help with the experiments.

References

(1) NASA/GSFC:Landsat4 to ground station interface discription ,Rev.6/7,1983.

(2) John L.Barker:Analysis of Multispectral Scanner(MSS) and Thematic Mapper(TM) performance,LTWG,1983.

(3) Proceeding of Landsat 4 early results symposium,1983.